

# Synthesis, morphology, and thermal behavior of polyrotaxanes composed of $\gamma$ -cyclodextrin and polydimethylsiloxanes

Narcisa Marangoci · Aurica Farcas · Mariana Pinteala · Valeria Harabagiu · Bogdan C. Simionescu · Tatiana Sukhanova · Maria Perminova · Anatolii Grigoryev · Galina Gubanova · Sergei Bronnikov

Received: 4 August 2008 / Accepted: 12 December 2008 / Published online: 10 January 2009  
© Springer Science+Business Media B.V. 2009

**Abstract** Epoxy-terminated polydimethylsiloxanes of two molecular weights ( $M_n$  about 1,250 and 2,100) were proved to undergo inclusion complexation into the inner cavity of  $\gamma$ -cyclodextrin, thus resulting in formation of polyrotaxanes. The supramolecular assembling, the structure, the morphology, and the thermal properties of polyrotaxanes were shown to depend on the polymer molecular weight, the molar ratio between the components, and the presence of free  $\gamma$ -cyclodextrin.

**Keywords** Polyrotaxanes ·  $\gamma$ -Cyclodextrin · Polydimethylsiloxane

## Introduction

Polyrotaxanes (PRots) are supramolecular inclusion complexes, which are composed of macrocycles (the host molecules) threaded onto linear macromolecules (the guest

molecules) [1, 2]. To build PRot inclusion complexes, cyclodextrins (CDs) are often used as the host molecules. The CD molecules are cyclic oligosaccharides having a truncated cylindrical cavity with a depth of ca. 7.9 Å. The inner hydrophobic cavity of CD molecule is capable to accommodate reagents of appropriate size and functionality, while the hydrophilic external surface confers aqueous solubility on the resulting inclusion complex. The internal diameter of the CD cavity varies from 5.7 to 9.5 Å, depending on the number of structural units in the macrocycle (6, 7, and 8 units for the first three members of the homologue series, i.e.  $\alpha$ -,  $\beta$ -, and  $\gamma$ -CDs) [3]. Linear components used to form PRots with CD usually have two hydrophilic end groups and a hydrophobic middle part. When both components of PRots are introduced in water, the hydrophobic parts of the linear polymer chains insert inside the CD cavity, while the hydrophilic parts stay outside the cyclic component. Thus, a driving force of the complexation here is the hydrophobic interaction between atoms in the polymer chain and the inner cavity of CD.

PRots are known to be perspective materials for their use in different technical applications, such as controlled molecular switchers [4], templates for generation of porous silica materials whose pore diameter depends on the pH values of the medium [5], oral drug delivery systems [6], etc. PRots can also be used for designing nanoscopic analogs of bearings, joints, motors, rotors, pistons, and macroscopic assemblies composed of interlocked mechanical parts [4]. Besides, PRots have also been proposed as ‘smart’ materials for sensors [7] and in data storage applications [8, 9].

The PRots synthesis based on the interaction of CDs and polydimethylsiloxane (PDMS) was first reported by Harada et al. [10, 11]. As the inner diameter of  $\alpha$ -CD is too small (5.7 Å), this lowest homologue does not allow the insertion of PDMS chains due to their large cross-section diameter.

---

Narcisa Marangoci, Valeria Harabagiu, Bogdan C. Simionescu were the Members of the European Polysaccharide Network of Excellence (EPNOE), <http://www.epnoe.eu>.

---

N. Marangoci · A. Farcas · M. Pinteala · V. Harabagiu · B. C. Simionescu  
“Petru Poni” Institute of Macromolecular Chemistry, Aleea Grigore Ghica Voda 41A, 700487 Iasi, Romania

B. C. Simionescu  
Department of Natural and Synthetic Polymers, “Gh. Asachi” Technical University, 700050 Iasi, Romania

T. Sukhanova · M. Perminova · A. Grigoryev · G. Gubanova · S. Bronnikov (✉)  
Russian Academy of Science, Institute of Macromolecular Compounds, Bolshoi Prospekt 31, 199004 St. Petersburg, Russia  
e-mail: bronnik@hq.macro.ru

However,  $\beta$ -CD was found to form inclusion complexes with PDMS of low molecular weight ( $M_n < 700$ ), while  $\gamma$ -CD was used to accommodate PDMS of  $M_n < 3,300$ . A maximum inclusion ratio of one CD molecule per 1.5 siloxane structural unit has also been established [10, 11].

In our previous publications [12, 13] we reported on the complexation of functionalized PDMS, namely glycidoxypropyl-terminated PDMS (E-PDMS), with  $\beta$ -CD. Polymers of two different molecular weights were checked and PRots containing  $\beta$ -CD molecules disposed only on the end organic moieties of the siloxane chains were obtained, denoting a difficult slipping of this macrocycle along the bulky siloxane chain. The structure, the morphology, and the thermal properties of those PRots were found to depend on PDMS molecular weight and on the content of free  $\beta$ -CD.

This paper gives a further insight in the structure-morphology-property relationship characterizing E-PDMS/CD inclusion complex by replacing the  $\beta$ -CD guest molecules with those of its higher homologue,  $\gamma$ -CD. Using the NMR spectra, we will give here the structural characterization of the obtained PRots. As the crystalline structure of  $\gamma$ -CD causes crystalline arrangement of the complexes, the WAXS method will be used to elucidate the type of the crystalline lattices of PRots. The expected dependence of PRot thermal behavior on the polymer molecular weight and on the presence of non-complexed  $\gamma$ -CD molecules will be proved by DSC method. The results on morphology investigation with SEM will be also presented. These data seem to be important since, next to chemical composition and reciprocal spatial arrangement of both polymer chains and CD molecules, the arrangement of supermolecular entities, i.e. morphology, is a key factor for understanding the material properties and functionality. Moreover, the comparison of these experimental findings with those obtained for PRots composed of PDMS and  $\beta$ -CD will evidence the influence of the structure of guest molecules on the morphology of inclusion complexes under investigation.

## Experimental

### Materials

Octamethylcyclotetrasiloxane ( $D_4$ ), 1,1,3,3-tetramethyldisiloxane (TMDS), and allyl glycidyl ether (AGE) (Aldrich) were used as received. Hexachloroplatinic acid (Aldrich) catalyst was used as 2% solution in isopropyl alcohol. Toluene, the hydrosilation solvent, was dried on calcium hydride and distilled before using.  $\gamma$ -CD (Aldrich) was dried under vacuum at 100 °C for 48 h. 4-aminophenyltriphenylmethane (APhTPhM), a bulky blocker of the PRot end groups, was prepared through the alkylation of acetanilide with triphenylmethane chloride, the separation

of the *para*-isomer through thin film chromatography, and the acid catalyzed hydrolysis of acetamide groups, following a procedure described in Ref. [14]. The solid yellowish product was purified by crystallization from methanol.

### Synthesis of $\alpha,\omega$ -bis(3-glycidoxypropyl)-polydimethylsiloxanes (E-PDMSs)

Linear polymers, E-PDMSs, of two molecular weights were prepared through cationic equilibration of  $D_4$  with 1,1,3,3-tetramethyldisiloxane (TMDS), followed by the hydrosilation of the obtained Si-H terminated polydimethylsiloxane (H-PDMS) with AGE in the presence of hexachloroplatinic acid catalyst, according to a method previously described [15]. The characteristics of polysiloxane precursors are presented in Table 1.

$^1\text{H-NMR}$ , ( $\text{CDCl}_3$ ),  $\delta$  (ppm):  $-0.04$  (s,  $\text{CH}_3\text{Si}$  end);  $-0.02$  and  $0.00$  (two s,  $\text{CH}_3\text{Si}$  chain);  $0.42$ – $0.48$  (m,  $\text{CH}_2\text{CH}_2\text{Si}$ ;  $\beta$  adduct);  $0.93$  (d,  $\text{CH}_3\text{-CHSi}$ ;  $\alpha$  adduct);  $1.10$  (q,  $\text{CH}_3\text{-CHSi}$ ;  $\alpha$  adduct);  $1.49$ – $1.58$  (m,  $\text{CH}_2\text{CH}_2\text{Si}$ ;  $\beta$  adduct);  $2.45$ – $2.47$  and  $2.63$ – $2.65$  (dd,  $\text{CH}_2$  epoxy);  $2.99$ – $3.00$  (m, CH epoxy);  $3.24$ – $3.40$  and  $3.56$ – $3.59$  (dd,  $\text{O-CH}_2\text{-epoxy}$  and m,  $\text{O-CH}_2\text{CH}_2\text{CH}_2\text{Si}$ ).

### PRots preparation

Saturated solutions of  $\gamma$ -CD in dimethylformamide (DMF) were mixed under vigorous stirring with E-PDMS at 65 °C till the solution become turbid (for about 72 h). The epoxy groups located at the ends of siloxane chains were then reacted with APhTPhM (saturated solution in isopropanol) (amino groups/epoxy groups = 1/1 molar ratio) for 8 h to create PRot structures. The obtained slurry solution was poured in cold water. The precipitate was filtrated, washed quickly with ethanol, dried (8 h at 40 °C), suspended overnight in diethyl ether to remove unreacted E-PDMS, filtered, and dried again for 8 h at 40 °C. The resulted crude samples (PRot<sub>c</sub>) contained a significant amount of free  $\gamma$ -CD. To completely remove the non-complexed  $\gamma$ -CD ( $\gamma$ -CD/siloxane ratio remained unchanged, as determined from  $^1\text{H-NMR}$  spectrum), twice precipitation from DMF/water system was required. Purified samples (PRot<sub>p</sub>) were obtained in quite high yields (more than 75%).

### Characterization

$^1\text{H-NMR}$  spectra of the intermediates and of PRots were obtained by using a Bruker DRX 400 MHz spectrometer with DMSO- $d_6$  as a solvent. The molecular weights and the polydispersity indexes of E-PDMSs and of PRots were determined by size exclusion chromatography (SEC) in chloroform and DMF, respectively, on a Water Associates

**Table 1** Characteristics of H-PDMS and E-PDMS

Sample code	Polymerisation degree of H-PDMS precursor <sup>a</sup>	Epoxy-groups content <sup>b</sup> (mol g <sup>-1</sup> )	$M_n$		$M_w/M_n$ SEC
			Chemical analysis	SEC <sup>c</sup>	
E-PDMS <sub>1</sub>	14.2	0.156	1,280	1,250	1.4
E-PDMS <sub>2</sub>	23.3	0.110	1,940	2,100	1.5

<sup>a</sup> Calculated from the integrals of the characteristic peaks for Si–H and Si–CH<sub>3</sub> groups at  $\delta = 4.7$  and 0.1 ppm in <sup>1</sup>H-NMR spectra

<sup>b</sup> Determined by potentiometric titration of epoxy groups with *p*-toluene sulfonic acid

<sup>c</sup> Solvent: CHCl<sub>3</sub>

440 instrument; polystyrene and polyethylene oxide standards were used for calibration curves. Wide angle X-ray diffraction (WAXD) analysis of  $\gamma$ -CD and PRot<sub>s</sub> was performed on a DRON-3 diffractometer (Burevestnik Research and Production Association, Russia) at scattering angles varying from 3 to 40° (CuK  $\alpha$ -radiation, Ni filter). The thermal properties of the samples were studied on a DSM 2 M calorimeter (Specialized Design Office for Instruments Production, Pushchino, Russia) at a scanning rate of 16 °C min<sup>-1</sup>. The morphology of the samples was observed by using a Akashi MINI-SEM-V scanning electron microscope (Japan).

## Results and discussion

### Synthesis of E-PDMS and PRot<sub>s</sub>

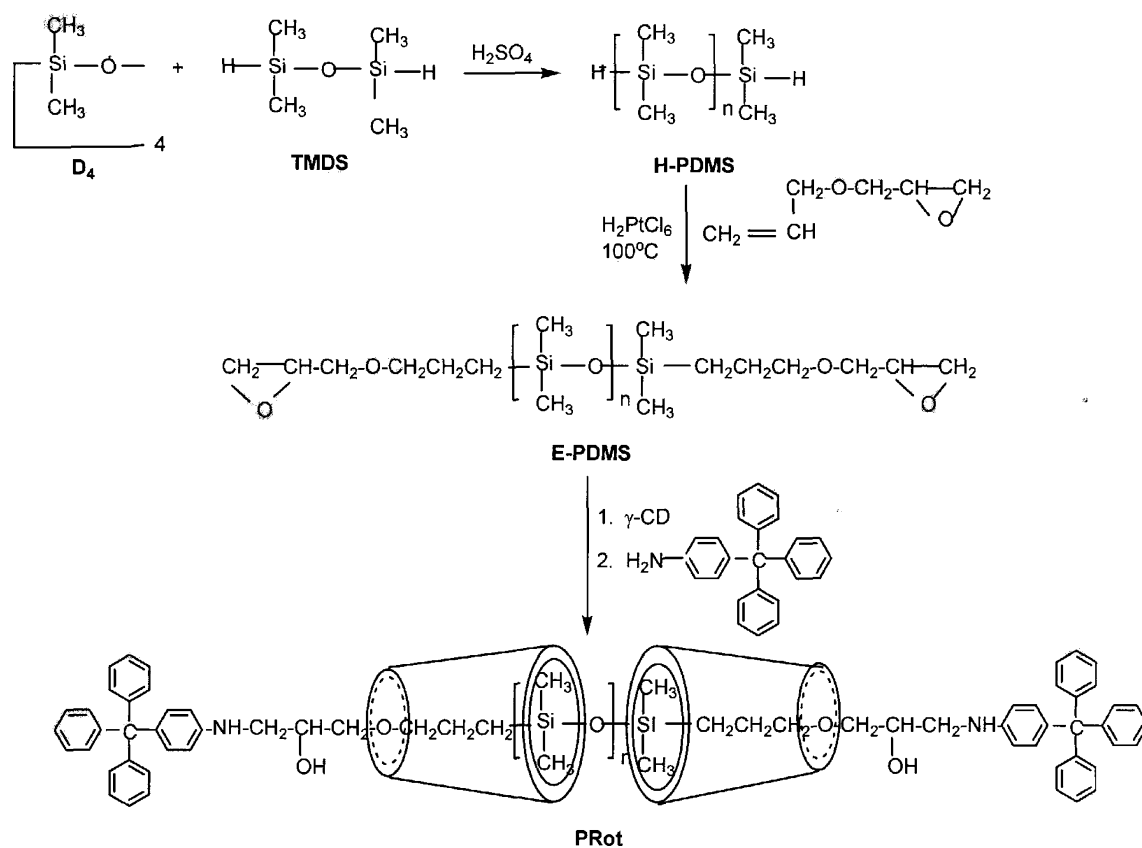
E-PDMSs with quite narrow molecular weight distributions were obtained by cationic equilibration of D<sub>4</sub> with TMDS, followed by the hydrosilation of the Si–H terminated precursors with AGE, according to a procedure described previously [15] (see Scheme 1). The <sup>1</sup>H-NMR spectra of E-PDMSs indicated that the hydrosilation undergoes mainly through the formation of  $\beta$ -adduct and only traces of  $\alpha$ -adduct were observed in the analyzed samples. To investigate the influence of the polymer chain length on the properties of the inclusion complexes, polymers of two different molecular weights,  $M_n$  about 1,250 and 2,100, were prepared (Table 1). The molecular weights of siloxane prepolymers were determined from <sup>1</sup>H-NMR spectra, chemical analysis, and SEC. As follows from Table 1, a good agreement between the results obtained by these methods was evidenced.

PRot<sub>s</sub> containing  $\gamma$ -CD threaded onto polysiloxane chains were obtained by mixing large excess of  $\gamma$ -CD with E-PDMSs in DMF, in a first step, and by stabilizing the formed pseudorotaxanes through the reaction of epoxy end groups with a bulky reagent, in a second step. The blocking reaction takes place in the colloidal dispersion of the pseudorotaxane. Both steps are shown in Scheme 1.

E-PDMS of both molecular weights,  $M_n$  about 1,250 and 2,100, were proved to undergo complexation with  $\gamma$ -CD. To determine the maximum inclusion ratio, a large excess of  $\gamma$ -CD was used for the preparation of the PRot samples. The precipitation of the reaction mixture and the extraction of the non-complexed polysiloxane in a selective solvent were performed to obtain the crude products (PRot<sub>c</sub>). Further, the crude products were carefully purified by twice reprecipitation of their DMF solutions in cold water (till no difference between  $\gamma$ -CD/SiO ratios was detected from <sup>1</sup>H-NMR spectra of the resulted purified PRot<sub>p</sub> samples). The yields registered for purified complexes were higher than 75%, as calculated against the initial amount of E-PDMS. Details on the synthesis and the composition of both crude and purified PRot samples are presented in Table 2.

### NMR data

The structure and the composition of both crude and purified PRot<sub>s</sub> were determined by NMR spectroscopy. Figure 1 presents the <sup>1</sup>H-NMR spectra of E-PDMS<sub>2</sub> and of PRot<sub>p</sub>-2100. In PRot<sub>p</sub>-2100, the methyl protons linked to the silicon atoms show quite different resonance peaks around 0 ppm as compared to the corresponding signals in the non-complexed E-PDMS precursor. The signal of the methyl protons linked to the end silicon atoms, appearing at –0.04 ppm in E-PDMS is shifted in a larger signal to lower magnetic field, at 0.05 ppm in PRot, while the methyl protons belonging to chain siloxane units are slightly up field to –0.07 ppm. The methylene protons linked in PRot<sub>p</sub>-2100 in  $\alpha$ - and  $\beta$ -positions to the silicon end atoms show less resolved and larger peaks as compared to the non-complexed siloxane. Moreover, the H<sup>1</sup> proton is moved from 4.85 ppm in native  $\gamma$ -CD to 4.90–4.98 ppm in PRot<sub>s</sub>. All these experimental findings evidence the inclusion of siloxane chain into  $\gamma$ -CD cavity. In the <sup>1</sup>H-NMR spectrum of PRot<sub>p</sub>-2100, the peaks corresponding to the epoxy groups at 2.45–2.47, 2.63–2.65 and 2.99–3.00 ppm disappeared due to the ring opening reaction with APhTPM end blocker. The newly formed CH<sub>2</sub>–NH and CH–OH groups give in the <sup>1</sup>H-NMR spectrum of PRot quite not resolved



**Scheme 1** Synthesis of  $\gamma$ -CD/E-PDMS inclusion complexes

**Table 2** Synthesis<sup>a</sup> and characterization of PRot samples

Reaction feed	Sample code	$\gamma$ -CD/SiO <sup>b</sup> (molar ratio)	PRots		$\gamma$ -CD content		Yield <sup>c</sup> (%)
			Sample code <sup>c</sup>	Sample content	$\gamma$ -CD/SiO <sup>b</sup> (molar ratio)	Free $\gamma$ -CD <sup>d</sup> (%)	
E-PDMS <sub>1</sub>		1.8	PRot <sub>c</sub> -1250	$\gamma$ -CD/E-PDMS <sub>1</sub> = 9/1 (PRot + free $\gamma$ -CD)	1/1.6	38	–
		1.8	PRot <sub>p</sub> -1250	$\gamma$ -CD/E-PDMS <sub>2</sub> = 5/1 (purified PRot)	1/2.8	0	81
E-PDMS <sub>2</sub>		1.8	PRot <sub>c</sub> -2100	$\gamma$ -CD/E-PDMS <sub>2</sub> = 15/1 (PRot + free $\gamma$ -CD)	1/1.6	46	–
		1.8	PRot <sub>p</sub> -2100	$\gamma$ -CD/E-PDMS <sub>2</sub> = 7/1 (purified PRot)	1/3.3	0	75

<sup>a</sup> Reaction conditions: (1) Pseudorotaxanes: stirring of  $\gamma$ -CD saturated solution in DMF with E-PDMS for about 72 h at 65 °C; (2) PRots: blocking with 4-aminophenyltriphenylmethane, NH<sub>2</sub>/epoxy = 1/1 molar ratio, 8 h at 65 °C

<sup>b</sup> Determined from <sup>1</sup>H-NMR spectra; SiO is dimethylsiloxane structural unit

<sup>c</sup> Purification conditions: PRot<sub>c</sub>-1250 and PRot<sub>c</sub>-2100 crude samples containing free  $\gamma$ -CD were obtained by precipitation of complexes in DMF/cold water system followed by washing with diethyl ether; PRot<sub>p</sub>-1250 and PRot<sub>p</sub>-2100 samples, containing pure PRots were obtained from crude samples by twice re-precipitation from DMF/water system

<sup>d</sup> Calculated considering  $\gamma$ -CD/polymer chain = 5/1 (PRot<sub>p</sub>-1250) and 7/1 (PRot<sub>p</sub>-2100)

<sup>e</sup> Calculated based on initial E-PDMS amount

peaks at around 3.16 and 3.72 ppm, respectively, while both doublets at 6.46–6.48 and 6.75–6.77 ppm and the multiplet between 7.05 and 7.35 ppm are belonging to the aromatic

protons of the end blocker. As in the region 3.3–3.6 ppm the CH<sub>2</sub>–O–CH<sub>2</sub> signals are superposed on those of CH<sup>2–6</sup> of the macrocycle, the ratio between  $\gamma$ -CD and siloxane units

was calculated using the integral of the  $H^1$  proton of  $\gamma$ -CD signal at 4.90–4.98 ppm and the sum of the integrals of the methyl-silicon signals around 0 ppm.

The calculation of the  $\gamma$ -CD content in the purified samples, PRot<sub>p</sub>-1250 and PRot<sub>p</sub>-2100, gives in average five and seven  $\gamma$ -CD molecules threaded onto each polymer chain, respectively, meaning a  $\gamma$ -CD/siloxane unit molar ratio of about 1/3 (Table 2). This is consistent with the idea that  $\gamma$ -CD, contrary to our previous findings for  $\beta$ -CD [12, 13], is able to undergo the threading not only on the end organic moiety, but also on the siloxane chains. The lower inclusion ratio as compared to the results of Harada et al. [10] could be explained by the partial dethreading of  $\gamma$ -CD molecules during the blocking reaction and/or by the PRot precipitation before accomplishing the maximum ratio of complexation. The last argument is also supported by the lower  $\gamma$ -CD/SiO molar ratio registered for PRot of higher siloxane molecular weight whose separation from the solution is expected to undergo more quickly.

To establish the influence of the polymer molecular weight, of  $\gamma$ -CD content in PRots, and of the presence of free  $\gamma$ -CD on the solid state behavior of PRots, both crude and purified samples with characteristics collected in Table 2 were further analyzed by using WAXS, DSC, and SEM methods.

#### WAXD data

WAXD patterns of  $\gamma$ -CD and PRots are shown in Fig. 2. All the patterns demonstrate tiny reflexes of different intensities; i.e. these samples have highly crystalline structures. The interplanar distances of the investigated samples are collected in Table 3.

The data obtained correlate with the results published in Refs. [16–21] where  $\gamma$ -CD [16–18] and the inclusion complexes of  $\gamma$ -CD with aromatic linear polymers [18], a biodegradable polymer [21], polyethylene oxide [19], and polyvinyl chloride [17] were studied. Following Refs. [16–18] one can conclude that  $\gamma$ -CD (Fig. 2, a) corresponds to the cage-type packing arrangement. Oppositely to  $\gamma$ -CD, all the PRot samples exhibit a characteristic peak at  $2\theta \approx 7.5^\circ$  (Fig. 2, b–e) indicating the formation of a crystalline inclusion complex of a channel structure, typical for other inclusion complexes [16–21]. The interplanar distances for PRot<sub>c</sub>-1250 and PRot<sub>p</sub>-1250 (see Table 3) are in agreement with the data published in Ref. [19] corresponding to the channel structure with a tetragonal packing. However, Fig. 2, d and e, related to PRot<sub>c</sub>-2100 and PRot<sub>p</sub>-2100 seems to be different from Fig. 2, b and c. Following the method published in Ref. [22], we found that PRot<sub>p</sub>-2100 has the cubic crystalline lattice with the unit cell parameters  $a = b = c = 14.8 \text{ \AA}$  (see Table 3), though the PRot<sub>c</sub>-1250

structure is formed by a mixture of both tetragonal and cubic crystals.

Thus, the crystalline structure of PRots is predetermined by the crystalline structure of  $\gamma$ -CD, though the types of the crystalline arrangements in  $\gamma$ -CD and PRots are different: cage and channel types, respectively. The molecular weight of the polymer, the molar ratio between the components, and the presence of non-complexed  $\gamma$ -CD is shown to influence the crystalline lattice packing in PRots: cubic or tetragonal.

#### DSC data

The influence of the polymer molecular weight and of the presence of non-complexed  $\gamma$ -CD on the thermal behavior of the PRots was investigated with the DSC method. Figure 3 presents the DSC curves related to  $\gamma$ -CD and PRot samples in air atmosphere. The thermogram of the pure  $\gamma$ -CD sample (Fig. 3, a) demonstrates a wide endo-thermal peak in the range of 50–170 °C with the maximum at 103 °C and with a low-temperature shoulder at 80 °C. The obtained result is in an agreement with the data published in Refs. [19, 20]. The main peak seems to be related to the evaporation of the complexed water, whereas the shoulder should rather be connected with the evaporation of the non-complexed water. At the second heating scan, this endo-thermal peak disappears. At higher temperature (about 280 °C),  $\gamma$ -CD melts and decomposes simultaneously.

A similar behavior (two endo-thermal effects) is typical for the PRot complexes of both molecular weights (Fig. 3, b–e). Their thermograms exhibit wide endo-thermal peaks in the range of 50–150 °C having a maximum value at about 100 °C. Above 270 °C, the PRot samples melt and decompose. The enthalpy values and the dehydration temperature maximum are listed in Table 4.

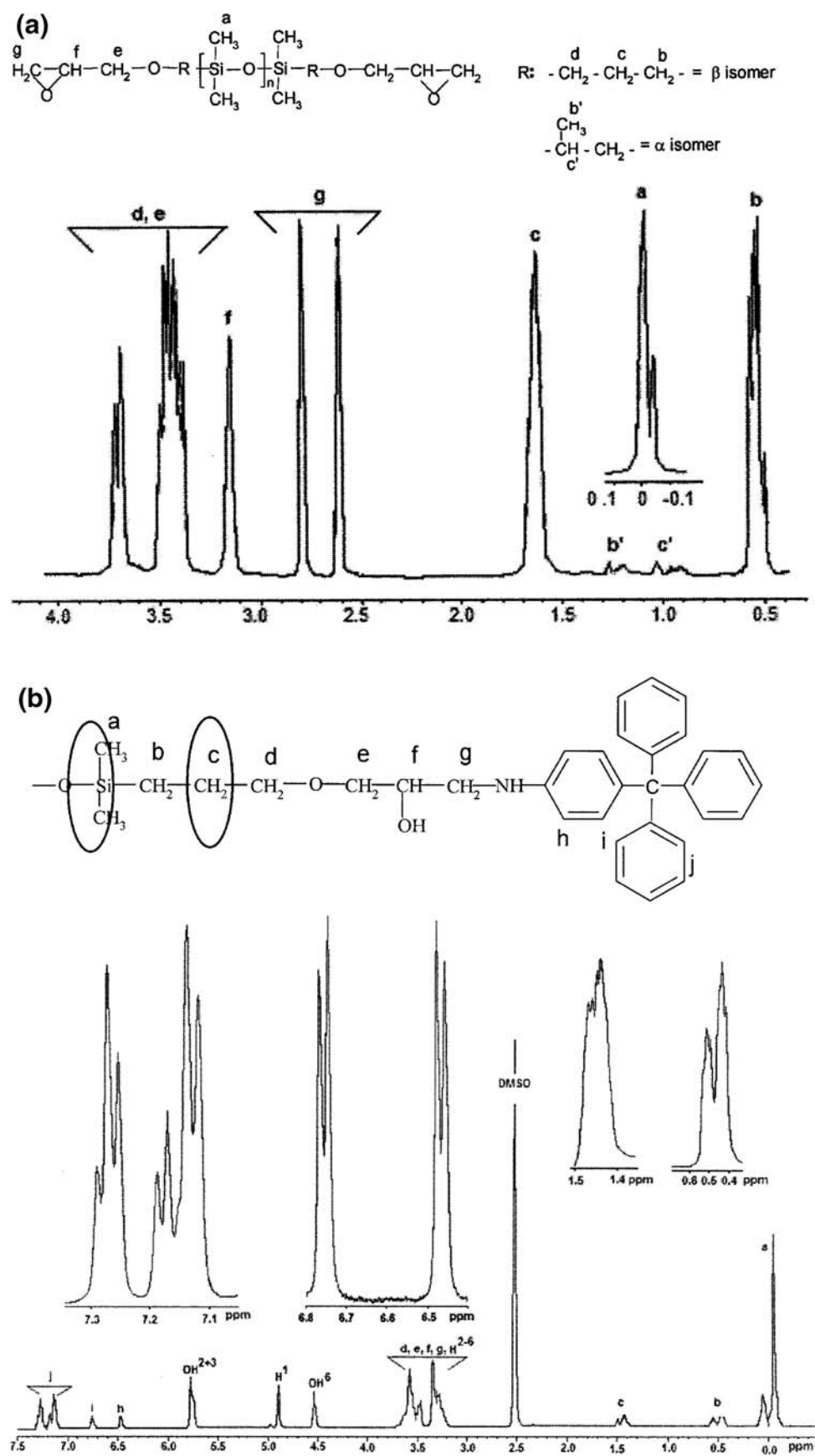
As follows from Table 4, the dehydration enthalpy values for the crude samples containing non-complexed  $\gamma$ -CD seem to be higher than those for purified PRots because of water excess. Yet, the maximum enthalpy value is typical for  $\gamma$ -CD with maximum water content.

#### SEM data

The SEM-images of  $\gamma$ -CD and PRots are presented in Fig. 4. As can be seen from Fig. 4a (low magnification), the morphology of  $\gamma$ -CD is formed by crystalline aggregates of irregular shape. Their length varies from 3 to 45  $\mu\text{m}$ , whereas their width varies from 2 to 12  $\mu\text{m}$ . In the micrograph, crystals of different modifications, rod-like crystalline grains and plate-like rhombic aggregates, can be recognized. At a higher magnification (Fig. 4b), a layered morphology of the main population of crystalline grains can be seen. The results of statistical analysis of the crystal



**Fig. 1**  $^1\text{H-NMR}$  spectra of (a) E-PDMS and (b) P $\text{R}_{\text{O}t\text{p}}$ -2100



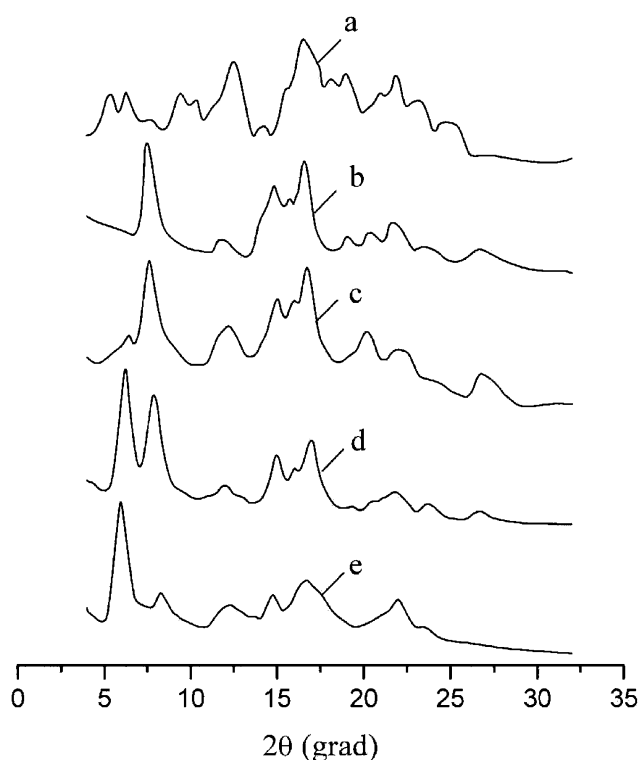


**Fig. 2** WAXS patterns of (a)  $\gamma$ -CD, (b) PRot<sub>c</sub>-1250, (c) PRot<sub>p</sub>-1250, (d) PRot<sub>c</sub>-2100, and (e) PRot<sub>p</sub>-2100

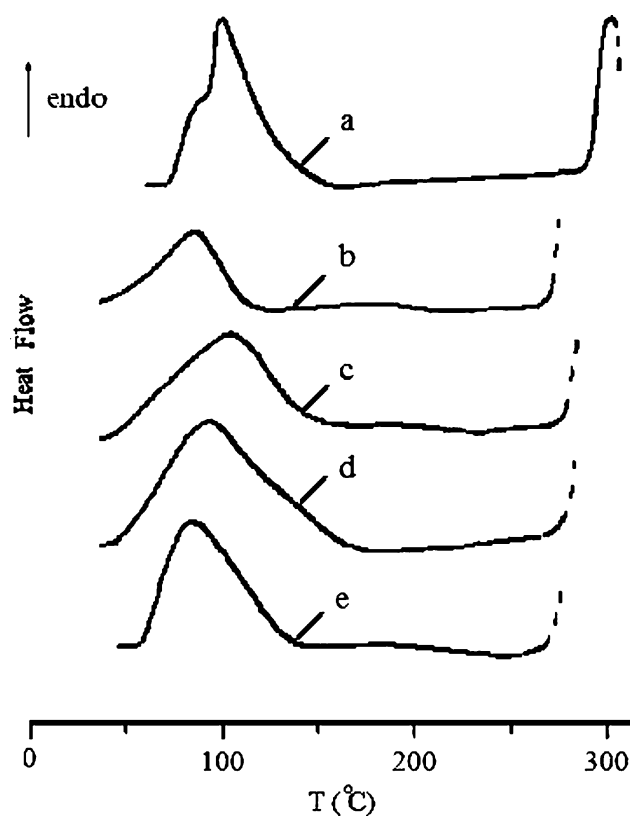


**Fig. 3** DSC data for (a)  $\gamma$ -CD, (b) PRot<sub>c</sub>-1250, (c) PRot<sub>p</sub>-1250, (d) PRot<sub>c</sub>-2100, and (e) PRot<sub>p</sub>-2100

size are presented in Fig. 5a and b, in the form of histograms described afterwards with the model of reversible aggregation [23, 24]. The mean grain length was estimated from the distribution curve as 21  $\mu\text{m}$  (Fig. 5a), whereas the mean grain width was found to be 5.8  $\mu\text{m}$  (Fig. 5b).

The morphology of the PRot<sub>c</sub>-1250 sample displays densely packed small aggregates of particles in the form of tetragonal parallelepipeds of both rectangular and square shapes (Fig. 4c), whereas the crystals of the PRot<sub>p</sub>-1250 sample have a plate-like lamellar morphology with a small number of rhombic crystals (Fig. 4d). At higher magnification, the stacked lamellae can be recognized.

The morphology of the PRot<sub>c</sub>-2100 sample is formed by large perfect cubic crystals (Fig. 4e). The statistical

**Table 4** DSC data for  $\gamma$ -CD and PRot samples

Sample code	$T_{\text{max}}$ (°C)	$\Delta H$ (J/g)
$\gamma$ -CD	103	237.5
PRot <sub>c</sub> -1250	90	224.1
PRot <sub>p</sub> -1250	95	160.0
PRot <sub>c</sub> -2100	100	206.9
PRot <sub>p</sub> -2100	85	156.0

analysis of the crystal edge size is presented in Fig. 5c. The mean edge of the cubes was estimated as 21  $\mu\text{m}$ . Finally, the micrograph of the PRot<sub>p</sub>-2100 sample is presented in Fig. 4g and h. Its morphology is formed by crystalline

**Table 3** Interplanar distances for  $\gamma$ -CD and PRots

Sample code	Interplanar distance (Å)
$\gamma$ -CD (experimental)	17.1 14.4 11.6 9.40 8.66 7.75 7.14 6.31 5.73 5.46 4.97 4.73 4.27 4.10 3.87 3.59
PRot <sub>c</sub> -1250 (experimental)	11.8 7.46 5.97 5.62 5.34 4.64 4.36 4.09 3.77 3.36
PRot <sub>p</sub> -1250 (experimental)	15.3 12.0 7.66 6.13 5.79 5.48 4.54 4.18 3.84 3.42 3.22
PRot <sub>c</sub> -2100 (experimental)	15.0 11.6 7.59 6.02 5.58 5.29 4.59 4.36 4.13 3.78 3.38
PRot <sub>p</sub> -2100 (experimental)	14.8 10.6 7.18 5.98 5.28 4.02
PRot <sub>p</sub> -2100 (calculated)	14.8 10.5 7.40 6.04 5.23 4.10

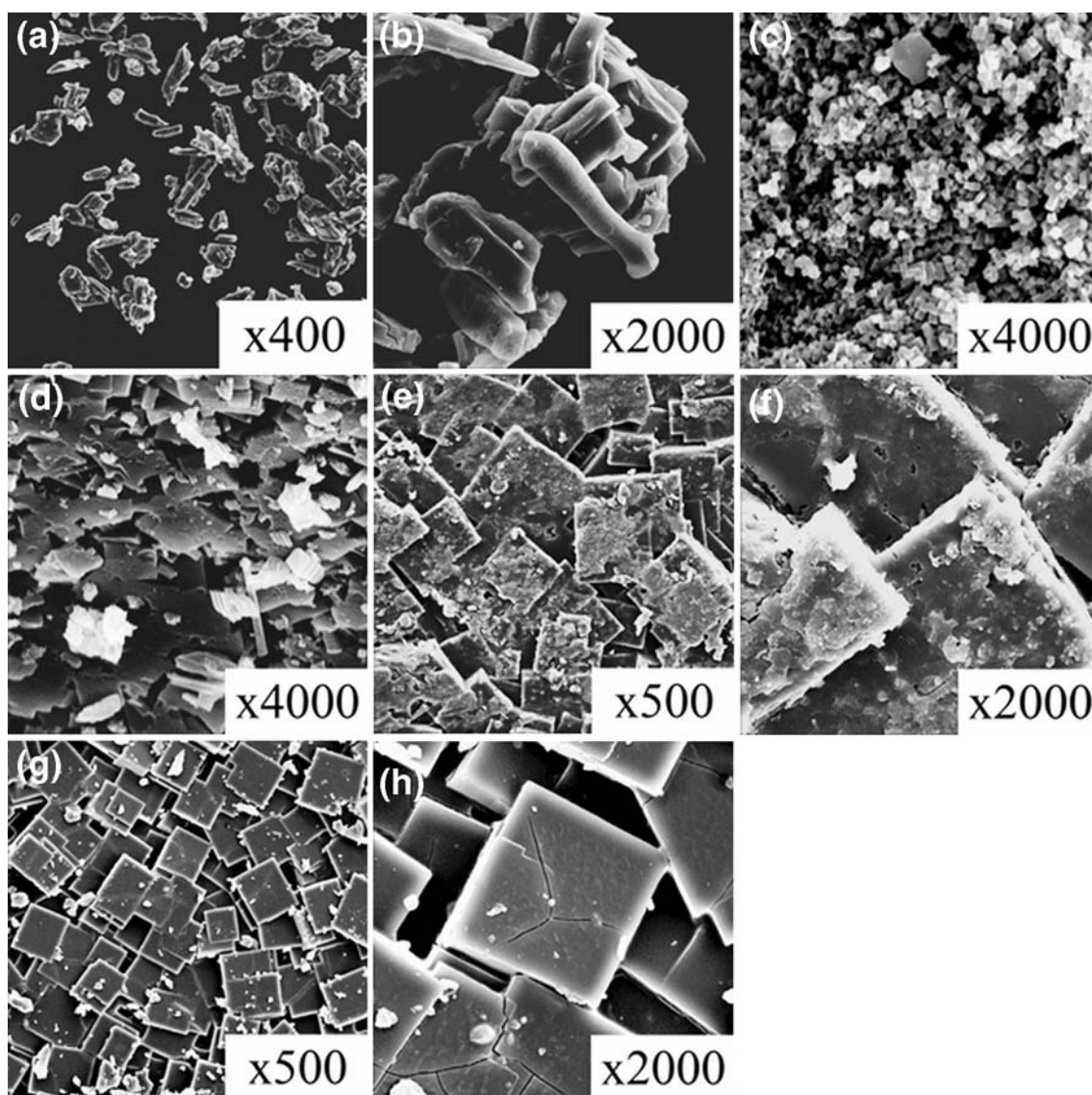


**Fig. 4** SEM images of (a, b)  $\gamma$ -CD, (c) PRot<sub>c</sub>-1250, (d) PRot<sub>p</sub>-1250, (e, f) PRot<sub>c</sub>-2100, and (g, h) PRot<sub>p</sub>-2100

cubes of regular shape; a mean edge of these crystals (Fig. 5d) was found to be as large as 65  $\mu\text{m}$ .

Thus, a correlation between the crystalline lattice packing of PProt and their morphology was evidenced by comparing WAXS, SEM, and statistical analysis data. Both molecular weight of the polymer and the presence of free  $\gamma$ -CD influence the morphology of the PProt samples.

We should note here that in our previous investigation of  $\beta$ -CD/E-PDMS complexes [12, 13], we observed quite different crystalline arrangements, e.g., rod-like crystals, stacked lamellae, and even amorphous structures. We can therefore conclude that the host molecule's structure also influences the PProt morphology.

## Conclusions

Glycidoxypropyl-terminated polysiloxanes of two molecular weights, 1,250 and 2,100, are shown to form inclusion complexes with  $\gamma$ -CD. As much as five to seven  $\gamma$ -CD molecules are proved to thread onto each polymer chain, respectively, giving an average  $\gamma$ -CD/siloxane structural unit molar ratio of about 1/3. The influence of both the length of the polymer chain and the  $\gamma$ -CD content on the morphology and the thermal behavior of the obtained inclusion complexes was sequentially analyzed. Moreover, a comparison with results obtained for PProt based on  $\beta$ -CD allowed establishing the correlations between structural,



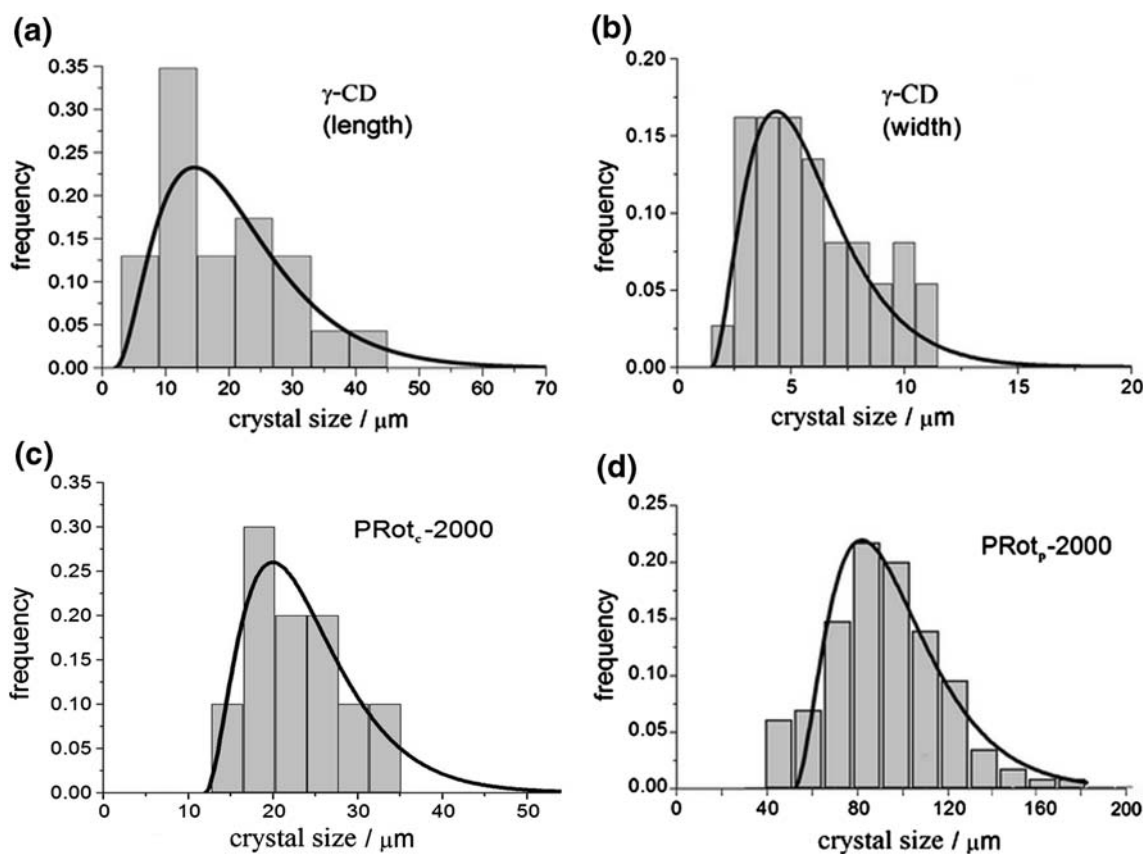


**Fig. 5** Statistical size distributions of the crystalline entities in (a, b)  $\gamma$ -CD, (c) PRot<sub>c</sub>-2100, and (d) PRot<sub>p</sub>-2100; their analytical description using the model of reversible aggregation [23, 24] is also presented

microscopic, and thermal properties of E-PDMS/CD inclusion complexes.

**Acknowledgements** Financial support of the Russian Foundation for Basic Research (project 07-03-91681) and of the Romanian Academy (project 3/2008) is gratefully acknowledged.

## References

- Schill, G.: Catenanes, Rotaxanes, and Knots. Academic Press, New York & London (1971)
- Huang, F., Gibson, H.W.: Polypseudorotaxanes and polyrotaxanes. *Prog. Polym. Sci.* **30**, 982–1010 (2005). doi:10.1016/j.progpolymsci.2005.07.003
- Szejtli, J.: Present, past, and future of cyclodextrin research. *Pure Appl. Chem.* **76**, 1825–1832 (2004). doi:10.1351/pac200476101825
- Balzani, V., Gumez-Lipez, M., Stoddart, J.F.: Molecular machines. *Acc. Chem. Res.* **31**, 405–411 (1998). doi:10.1021/ar970340y
- Han, B.H., Antonietti, M.: Cyclodextrin-based pseudorotaxanes as templates for the generation of porous silica. *Chem. Mater.* **14**, 3477–3488 (2002). doi:10.1021/cm0113088
- Ooya, T., Eguchi, M., Ozaki, A., Yui, N.: Carboxyethyl ester-polyrotaxanes as new calcium binding and mechanism of trypsin inhibition. *Int. J. Pharm.* **242**, 47–52 (2002). doi:10.1016/S0378-5173(02)00139-4
- Lee, J.Y., Park, S.M.: Electrochemistry of guest molecules in thiolated cyclodextrin self-assembled monolayers: an application for size-selective sensors. *J. Phys. Chem. B* **102**, 9940–9945 (1998). doi:10.1021/jp9828235
- Balzani, V., Credi, A., Raymo, F.M., Stoddart, J.F.: Artificial molecular machines. *Angew. Chem. Int. Ed.* **39**, 3348–3391 (2000). doi:10.1002/1521-3773(20001002)39:19<3348::AID-ANIE3348>3.0.CO;2-X
- Hubin, T.J., Busch, D.H. Templates routes to interlocked molecular structures and orderly molecular entanglements. *Coord. Chem. Rev.* **200–202**, 5–52 (2000) doi: 10.1016/S0010-8545(99)00242-8
- Okumura, H., Okada, M., Kawaguchi, Y., Harada, A.: Complex formation between poly(dimethylsiloxane) and cyclodextrins: new pseudo-rotaxanes containing inorganic polymers. *Macromolecules* **33**, 4297–4298 (2000). doi:10.1021/ma991934e
- Okumura, H., Kawaguchi, Y., Harada, A.: Complex formation between poly(dimethylsilane) and cyclodextrins. *Macromol. Rapid Commun.* **23**, 781–785 (2002). doi:10.1002/1521-3927(20020901)23:13<781::AID-MARC781>3.0.CO;2-C
- Sukhanova, T., Bronnikov, S., Grigoryev, A., Gubanov, G., Perminova, M., Marangoci, N., Pinteala, M., Harabagiu, V., Simionescu, B.C.: Synthesis, structure, and thermal properties of polyrotaxanes derived from  $\beta$ -cyclodextrin. *Russ. J. Appl. Chem.* **80**, 1111–1115 (2007). doi:10.1134/S1070427207070191
- Marangoci, N., Farcas, A., Pinteala, M., Harabagiu, V., Simionescu, B.C., Sukhanova, T., Bronnikov, S., Grigoryev, A., Gubanov, G., Perminova, M., Perichaud, A.: Polyrotaxanes composed of  $\beta$ -cyclodextrin and polydimethylsiloxanes:

- synthesis, morphology and thermal behavior. *High Perform. Polym.* **20**, 251–266 (2008). doi:[10.1177/0954008307079538](https://doi.org/10.1177/0954008307079538)
14. Witten, B., Reid, E.E.: *Organic Synthesis*, vol. 4, pp. 47–63. Wiley, New York & London (1963)
  15. Harabagiu, V., Pinteala, M., Cotzur, C., Holerca, M.N., Ropot, M.J.: Functional polysiloxanes: 3. Reaction of 1,3-bis(3-glycidoxypropyl)-1,1,3,3-tetramethyldisiloxane with amino compounds. *J. Macromol. Sci. A* **32**, 1641–1648 (1995)
  16. Uyar, T., Hunt, M.A., Gracz, H.S., Tonelli, A.E.: Crystalline cyclodextrin inclusion compounds formed with aromatic guests: guest-dependent stoichiometrics and hydration-sensitive crystal structures. *Cryst. Growth Des.* **6**, 1113–1119 (2006). doi:[10.1021/cg050500+](https://doi.org/10.1021/cg050500+)
  17. Martinez, G., Gomez, M.A., Tonelli, A.E.: Formation of crystalline inclusion complexes of poly(vinyl chloride) with  $\gamma$ -cyclodextrin. *Proceedings 41st International Symposium on Macromolecules*, p. 118. Rio de Janeiro, Brazil, 16–21 July 2006
  18. Shuai, X., Porbeni, F.E., Wei, M., Bullions, T., Tonelli, A.E.: Inclusion complex formation between  $\alpha$ ,  $\gamma$ -cyclodextrins and triblock copolymer and the cyclodextrin-type-dependent micro-phase structures of their coalesced samples. *Macromolecules* **35**, 2401–2405 (2002). doi:[10.1021/ma012085+](https://doi.org/10.1021/ma012085+)
  19. Panova, I.G., Gerasimov, V.I., Tashlitsky, V.N., Topchieva, I.N., Kabanov, V.A.: Crystalline inclusion complexes based on cyclodextrins and triblock copolymers of ethylene and propylene oxides. *Polym. Sci. A* **39**, 452–458 (1997)
  20. Panova, I.G., Matukhina, E.V., Popova, E.I., Gerasimov, V.I., Topchieva, I.N.: Structure of inclusion complexes of  $\beta$ -cyclodextrin with poly(propylene oxide). *Polym. Sci. A* **43**, 771–777 (2001)
  21. Guo, J., Sun, J., Cao, H., Yang, H.: Inclusion complexes of cholesteryl-( $\epsilon$ -caprolactone)-functionalized polymer with  $\gamma$ -cyclodextrin. *J. Incl. Phenom.* **60**, 95–101 (2002)
  22. Ahmed, F.R., Hall, S.R., Huber, C.P.: *Crystallographic Computing*. Munksgaard, Copenhagen (1970)
  23. Kilian, H.G., Metzler, R., Zink, B.: Aggregate model of liquids. *J. Chem. Phys.* **107**, 8697–8704 (1997). doi:[10.1063/1.475022](https://doi.org/10.1063/1.475022)
  24. Kilian, H.G., Bronnikov, S., Sukhanova, T.: Transformations of the micro-domain structure of polyimide films during thermally induced chemical conversion: characterization via thermodynamics of irreversible processes. *J. Phys. Chem. B* **107**, 13575–13582 (2003). doi:[10.1021/jp035074m](https://doi.org/10.1021/jp035074m)